

Molecular and crystal structure of poly(tetramethylene adipate) α form based on synchrotron X-ray fiber diffraction

Keiichi Noguchi^{a,*}, Hidekazu Kondo^b, Yasushi Ichikawa^{b,1},
Kenji Okuyama^{b,2}, Junichiro Washiyama^c

^aInstrumentation Analysis Center, Tokyo University of Agriculture and Technology, 2-24-16 Naka-cho, Koganei, Tokyo 184-8588, Japan

^bFaculty of Technology, Tokyo University of Agriculture and Technology, Koganei, Tokyo 184-8588, Japan

^cSunAllomer, Ltd, Kawasaki Development Center, 2-3-2 Yako, Kawasaki-ku, Kawasaki 210-0863, Japan

Received 10 June 2005; received in revised form 22 August 2005; accepted 3 September 2005

Available online 22 September 2005

Abstract

The molecular and crystal structure of the α form of poly(tetramethylene adipate) (PTMA) was analyzed using synchrotron X-ray fiber diffraction data. The crystals belong to the monoclinic system of space group $P2_1/n$. The unit cell constants are $a=0.6776(6)$, $b=0.7904(6)$, c (fiber axis) = 1.442(1) nm and $\beta=135.6(1)^\circ$. The final crystal structure was obtained by the linked-atom least-squares refinement, which gave an R -factor of 0.130 for 103 observed spots and 64 unobserved reflections. The molecular structure deviates slightly from the fully extended conformation in the ester part. The torsional angle $\text{CH}_2\text{--CH}_2\text{--O--C(=O)}$ was found to be 155° . The C=O groups of the corner and center chains in a unit cell are closely located along the c -axis and are related by the crystallographic 2_1 -axes along the b -axis at $z=1/4$ and $z=3/4$. The total dipole moment arising from the C=O groups is oriented in one direction at $z=1/4$, and in the opposite direction at $z=3/4$. Owing to the close arrangement of the C=O groups between neighboring chains along the fiber axis, the c -projected cell dimensions and the setting angle of the polymer chain are different from those of the orthorhombic form of polyethylene and the β form of PTMA.

© 2005 Elsevier Ltd. All rights reserved.

Keywords: Crystal structure; Polyester; Synchrotron radiation

1. Introduction

With the increasing concern over pollution caused by plastic wastes, many approaches have been proposed for solving this problem, such as recycling and using biodegradable plastic materials. Aliphatic polyesters are typical polymers with great potential for use as biodegradable plastic, owing to their susceptibilities to degradation by lipases and esterases in microorganisms distributed widely in natural environments [1–5]. Poly(ethylene succinate) (PES), poly(tetramethylene succinate) (PTMS), and poly(tetramethylene adipate) (PTMA) are biodegradable synthetic aliphatic polyesters. PTMS and poly(tetramethylene succinate-*co*-adipate) have been commercialized under the trademark of

BIONOLLE® and their applications are growing [6,7]. Hence, fundamental studies are necessary to improve and develop such aliphatic polyesters.

In our previous studies [8–12], the polymorphisms, crystal structures and solid-state crystal transition mechanism of PTMS and PES were investigated. PTMA also exhibits polymorphisms and has at least two crystal forms (α and β forms) [13,14]. Minke and Blackwell [13,14] reported that samples of the α and β forms of PTMA could be obtained by annealing a stretched film at 52°C for several days and by stretching a quenched film, respectively. Furthermore, a spontaneous crystal transition from the β form to the α form was observed at room temperature. Recently, Gan et al. [15,16] found that crystals of the α form, β form, and a mixture of the two grew at crystallization temperatures above 32°C , below 27°C , and between these two temperatures, respectively. Although no obvious structural change of crystals of the β form was found at the crystallization temperature, the solid-state transition from β to α form took place at a sufficiently high annealing temperature. The equilibrium melting temperature (T_m^0) of each crystal form was determined based on Hoffman–Weeks and Gibbs–Thomson equations [16]. The T_m^0 of the α

* Corresponding author. Tel.: +81 42 388 7188; fax: +81 42 388 2041.

E-mail address: knoguchi@cc.tuat.ac.jp (K. Noguchi).

¹ On leave from Showa Denko K.K. Kawasaki Plastics Laboratory.

² Present address: Graduate School of Science, Osaka University, Toyonaka, Osaka 560-0043, Japan.

form was found to be higher than that of the β form, indicating that the α form was thermodynamically stable. However, crystals of the α form showed a faster enzymatic degradation than those of the β form [17]. The disparity in biodegradability would reflect the differences of intermolecular interaction, chain mobility, surface structure and morphology between the two forms. In fact, ^{13}C spin-lattice relaxation time analysis has revealed that molecules in the crystalline portion of the β form of PTMA were less mobile than those in the α form [18]. For a better understanding of the thermal and mechanical properties, biodegradability, processability, molecular motion and stability of these crystal forms, it is important to determine solid-state structures at a molecular level.

Minke and Blackwell [13,14] proposed unit cell parameters of $a=0.673(1)$, $b=0.794(1)$, c (fiber axis) $=1.420(4)$ nm and $\beta=45.5(1)^\circ$, and a possible space group of $P2_1/a$ for the α form of PTMA using 34 reflections obtained from the X-ray and electron diffraction data. In the fiber diffraction pattern of the β form, they observed discrete reflections on the equator and streaks on the other layer lines. Since, these results suggested that the β form contained disorder along the fiber axis, c -projected unit cell dimensions of $a'=0.5062(5)$, $b'=0.7325(9)$ nm and $\gamma'=90^\circ$, and fiber period of 1.465 nm were reported. However, no details on chain packing in the two crystal forms were provided [13,14].

Recently, Pouget et al. [19] analyzed the crystal structures of both the α and β forms of PTMA. For the α form, a chain conformation distorted from the fully extended structure and the space group $P2_1/n$ were deduced from the electron diffraction data up to a resolution of 0.15 nm obtained from solution-grown single crystals, together with the X-ray fiber diffraction data at 0.21 nm from stretched-annealed fibers. In their model, the conformation at $\text{CH}_2\text{-CH}_2\text{-O-C(=O)}$ was nearly skew. The final packing model of the α form was refined using 11 equatorial $hk0$ reflections from the electron diffraction pattern and gave a crystallographic R -factor of 0.19. In the case of the β form, they proposed a molecular structure with the all-trans conformation and polyethylene-like molecular packing projected along the c -axis based on the equatorial electron diffraction data.

In a more recent study using X-ray and electron diffraction, Iwata et al. [20] found essentially the same c -projected structure of the β form. Although they observed data at a resolution of 0.20 nm (19 independent spots) from annealed fibers of the α form, a detailed structure analysis on the α form was not performed. On the other hand, the authors independently analyzed the crystal structure of the α form using 31 independent spots from the equator to the sixth layer line (0.18 nm resolution) and proposed the same space group $P2_1/n$ [21]. However, in our model, the molecular structure deviated less from the fully extended structure than that proposed by Pouget et al. [19].

In order to yield precise structural information on PTMA, the authors attempted to obtain fiber diffraction data at a higher resolution using a synchrotron radiation source and reexamined the crystal structure of the α form.

2. Experimental section

2.1. Sample preparation

The PTMA sample was supplied by Showa Highpolymer Co. Ltd, and used without further purification. The weight average molecular weight was determined to be 7.07×10^4 by size exclusion chromatography with poly(methylmethacrylate) standards. The melting and glass transition temperatures of PTMA were measured by differential scanning calorimeter and found to be 59 and -55°C , respectively. Uniaxially oriented samples were prepared by slow cooling of molten samples, followed by stretching to about five times the original length at room temperature. The α form samples for the X-ray measurements were obtained by annealing the oriented samples at 45°C for a few weeks at a constant length. The diameter of these fibers was about 500 μm . The density of the sample was determined by the flotation method with densities of liquid media (NaCl aqueous solution) measured using a pycnometer.

2.2. X-ray measurements

X-ray measurements were carried out using synchrotron radiation (wave length = 0.07293 nm) at beam line BL40B2 of SPring-8, Hyogo, Japan. Fiber diffraction patterns of the α form of PTMA were recorded using a camera system equipped with a flat imaging plate (R -AXIS IV⁺⁺, Rigaku) at room temperature. The camera distance (150 mm) was calibrated with the characteristic d -spacings of Si powder. X-ray intensities and d -spacings of diffraction spots were obtained using in-house data processing software [22–24]. The observed intensities were corrected with the Lorentz-polarization factor [25]. No absorption correction was made in this study.

2.3. Structure analysis

Molecular and crystal structure models were constructed and refined using the linked-atom least-squares (LALS) technique [26]. At each stage of the modeling and refinement, the quantity Ω was minimized in the following least-squares fashion.

$$\Omega = \sum_m w_m (|F_m^o| - |F_m^c|)^2 + \sum_i k_i (d_i - d_i^o)^2 + \sum_j e_j (p_j - p_j^o)^2 + \sum_q \lambda_q G_q \quad (1)$$

The first term represents the differences between the observed $|F_m^o|$ and calculated $|F_m^c|$ structure amplitudes. In the present study, the reflections below the observed threshold were also included in the structure analysis. The unobserved reflections within the highest observed diffraction angle were assumed to have two-thirds of the intensity of the weakest observed reflection. The weight factor, w_m , was chosen to be 1.0 for the observed reflections. For the unobserved reflections, on the other hand, $w_m = 1.0$ when $|F_m^c| \geq |F_m^o|$, while $w_m = 0$ when

$|F_m^c| < |F_m^o|$. To prevent unreasonably close interatomic contacts in the crystal structure models, the second term are included in the least-squares optimization. This term adjusts the non-bonded interatomic distances (d_i) to their normally accepted values. The contact limits (d_i^o) of 0.360 (for C···C), 0.342 (C···O), 0.310 (C···H), 0.324 (O···O), 0.292 (O···H) and 0.260 (H···H) nm were used in this study. The third term is used to restrain certain parameters or quantities (p_j), such as torsional angles and bond angles, to their expected values found in surveys of known structures (p_j^o). The weights k_i are chosen to match non-bonded interatomic potentials and the weights e_j are inversely proportional to the variance of the values observed in the crystal structure. The last term imposes exact mathematical condition that enables one or more least-squares variables to be expressed exactly in terms of other variables (constrain). Certain constrains, such as continuity of chains and direct linear relations between varied parameters derived from crystallographic symmetry, are satisfied when $G_q=0$, and the λ_q are Lagrange multipliers.

In this study, the evaluation of the packing structure was done using the conventional (R_c) and weighted (R_w) R -factors defined in Eqs. (2) and (3), respectively.

$$R_c = \frac{\sum_m w_m ||F_m^o| - |F_m^c||}{\sum_m w_m |F_m^o|} \quad (2)$$

$$R_w = \left[\frac{\sum_m w_m (|F_m^o| - |F_m^c|)^2}{\sum_m w_m |F_m^o|^2} \right]^{1/2} \quad (3)$$

Atomic scattering factors for calculating structure factors were obtained by using the method and values given in the literature [27]. Computations were carried out on a PC using the WinLALS program version 1.109 [28].

3. Crystal structure analysis

The X-ray fiber diffraction pattern of the α form is shown in Fig. 1. A total of 103 independent diffraction spots were observed from the equator to the 12th layer line. Compared to all the previous studies [13,14,19–21], higher resolution reflection data up to a resolution of 0.11 nm were recorded using the synchrotron radiation source. The small variations in conformation and chain packing can thus be identified based on the synchrotron data. All the observed reflections in Fig. 1 could be indexed in terms of a monoclinic cell with parameters of $a=0.6776(6)$, $b=0.7904(6)$, c (fiber axis) = 1.442(1) nm and $\beta=135.6(1)^\circ$. Although a slightly longer fiber period was obtained in the present study, this unit cell is essentially the same as those reported previously [13,14,19–21]. The observed fiber period of 1.442 nm is close to the expected value of the all-trans conformation model (1.449 nm), in which there is one chemical repeating unit. The fully extended model could thus be adopted at the initial stage of our analysis. Bond lengths and bond angles used in molecular model building and the definition of the bond angles and torsional angles, together with atomic numbering, are shown in Fig. 2. Standard bond lengths and

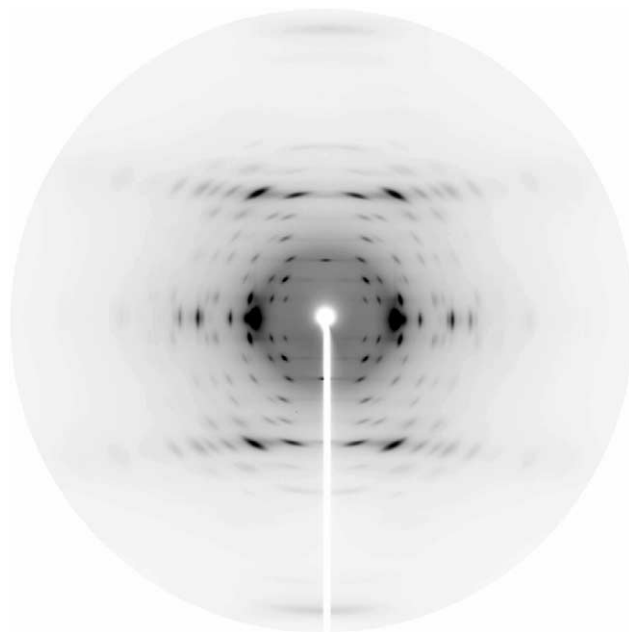


Fig. 1. Fiber diffraction pattern of the α form of poly(tetramethylene adipate) (PTMA).

angles were retrieved from the Cambridge Structure Database [29] on the basis of a search for X-ray structures containing a C–CH₂–O–C(=O)–CH₂–CH₂–C fragment with a crystallographic R factor of ≤ 0.075 . The hydrogen atoms attached to methylene carbons were introduced using a C–H bond length of 0.109 nm and C–C–H bond angle of 109.5°. The unit cell obtained in this study gives a calculated density of 1.23 g cm⁻³ comparable to the observed density of 1.18 g cm⁻³ when it contains two chemical repeating units (two polymer chains).

Because of the spread of diffraction spots, the accidental overlap due to cylindrical averaging, and the limitations of the resolution of the fiber diffraction pattern, the space group could not be unequivocally determined based on systematic extinctions of reflections. At first, the plane group of the c -projected structure was examined. Among the seven rectangular plane groups pm , pg , cm , $p2mm$, $p2mg$, $p2gg$

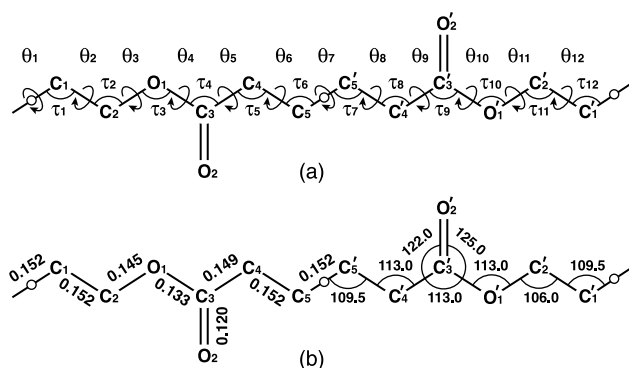


Fig. 2. (a) Atomic numbering scheme and the definition of the bond angles and torsional angles, together with (b) standard bond lengths (nm) and angles (°) used in this study. Open circles indicate inversion centers.

and $c2mm$ [30], both cm and $c2mm$ could be rejected in terms of the existence of a 120 reflection, which showed a relatively strong diffraction intensity. The c -projected structures assigned to the above five plane groups were thus analyzed by using 13 observed and 10 unobserved equatorial $hk0$ reflections. The R -factors of the c -projected (two dimensional) models with the symmetry of pm , $p2mm$ and $p2mg$ were found to be substantially high ($R > 0.30$) compared with those of pg and $p2gg$ ($R \approx 0.11$). It was also found that in the case of pg , the polymer chains were located approximately $0.25b$ (a -glide) or $0.25a$ (b -glide) apart from the respective glide plane. This observation indicated that the two-dimensional models assigned to pg and $p2gg$ were essentially the same. The plane group $p2gg$ was thus adopted. The space groups having the symmetry of $p2gg$ in a monoclinic system (b -unique) are $P2_1/a$ and $P2_1/n$ [30]. In addition, the space group $P2_1$ also has this symmetry when a polymer chain is located at $x=0.25$.

In the next step, a three-dimensional structure was analyzed using all the 103 observed and 64 unobserved X-ray data. Since, the centers of symmetry in the chemical repeating unit (the midpoints of the C1–C1' and C5–C5' bonds) must coincide with the crystallographic inversion centers [(0,0,0) and (0,0,0.5)], the location of molecules in the unit cell can be uniquely obtained in the cases of both $P2_1/a$ and $P2_1/n$. The azimuthal angle of the polymer chain around the molecular axis, together with the scale factor and the overall attenuation factor were then optimized. After refinement, the packing models for the space groups $P2_1/a$ and $P2_1/n$ showed $\Omega = 5.32 \times 10^4$ and $R_w = 0.312$, and $\Omega = 3.61 \times 10^4$ and $R_w = 0.249$, respectively. When polymer chains are allowed to translate along the c -axis, the packing models have the symmetry of space group $P2_1$ still keeping the same c -projected structure. Hence, crystal structure models with the symmetry of $P2_1$ were also examined. Although the translation of the polymer chains along the c -axis can be included in the refined parameters, the lowest R -factor was obtained for the packing model similar to that having the $P2_1/n$ symmetry. Therefore, space group $P2_1$ was not considered in the following analysis. As long as the fully extended model was used, the R -factors were not improved below 0.249.

In the final step, the chain conformation was optimized by varying bond and torsion angles under the constraints of the continuity of a polymer chain. Because of the two inversion centers in a chemical repeating unit, the bond and torsion angles should be $\tau_1 = \tau_{12}$, $\tau_2 = \tau_{11}$, $\tau_3 = \tau_{10}$, $\tau_4 = \tau_9$, $\tau_5 = \tau_8$, $\tau_6 = \tau_7$, $\theta_1 = \theta_7 = 180^\circ$, $\theta_2 = -\theta_{12}$, $\theta_3 = -\theta_{11}$, $\theta_4 = -\theta_{10}$, $\theta_5 = -\theta_9$ and $\theta_6 = -\theta_8$. Accordingly, there were eleven conformational parameters ($\tau_1, \tau_2, \tau_3, \tau_4, \tau_5, \tau_6, \theta_2, \theta_3, \theta_4, \theta_5$ and θ_6) in an asymmetric unit. The bond angles were restrained to their initial values used in the model building. After further refinement under the above constraining and restraining conditions, the Ω and R_w of the packing model for $P2_1/a$ were little improved ($\Omega = 4.46 \times 10^4$ and $R_w = 0.284$). On the other hand, those of the packing model for $P2_1/n$ were improved to 1.01×10^4 and 0.130, respectively.

Table 1
Final refinement parameters of the α form of PTMA

| | |
|---|------------|
| Torsional angle (°) | |
| θ_2 | −178.2(7) |
| θ_3 | −155.2(14) |
| θ_4 | −174.0(7) |
| θ_5 | −174.7(13) |
| θ_6 | −178.4(7) |
| Bond angle (°) | |
| τ_1 | 108.5(7) |
| τ_2 | 105.8(5) |
| τ_3 | 111.1(6) |
| τ_5 | 115.5(6) |
| τ_6 | 109.5(5) |
| Scale factor | 0.465(8) |
| Attenuation factor | 7.4(3) |
| Eulerian angle (°) | |
| ε_x | −97.1(6) |
| ε_y | −52.7(6) |
| ε_z | −34.9(10) |
| Azimuthal angle (°) | |
| μ | 174(1) |
| R-factor | |
| R | 0.162 |
| R_w | 0.130 |
| $R(\text{ex})^a$ | 0.154 |
| $R_w(\text{ex})^a$ | 0.127 |
| No. of reflections used in the refinement | |
| Observed spots | 103 |
| Unobserved reflections | 64 |

^a R -factor was calculated excluding unobserved reflections.

In addition, the shortest non-bonded interatomic distance in both models was 0.205 nm ($P2_1/a$, between O2 and H2a) and 0.232 nm ($P2_1/n$, between H1b and H5b), respectively. These results indicate that the crystal structure model assigned to $P2_1/n$ was preferable to the α form of PTMA. The final refined parameters and fractional atomic coordinates are listed in Tables 1 and 2. The packing structures are shown in Fig. 3. A comparison between observed and calculated structure factors is given as supplementary data.

Table 2
Final fractional atomic coordinates of the α form of PTMA

| Atom | x | y | z |
|------|--------|--------|-------|
| C1 | 0.059 | −0.035 | 0.565 |
| C2 | −0.034 | 0.079 | 0.613 |
| C3 | −0.054 | 0.051 | 0.764 |
| C4 | 0.085 | −0.002 | 0.899 |
| C5 | −0.085 | 0.028 | 0.930 |
| O1 | 0.093 | 0.009 | 0.738 |
| O2 | −0.275 | 0.125 | 0.689 |
| H1a | −0.020 | −0.163 | 0.550 |
| H1b | 0.289 | −0.038 | 0.639 |
| H2a | 0.040 | 0.208 | 0.627 |
| H2b | −0.263 | 0.079 | 0.543 |
| H4a | 0.128 | −0.137 | 0.906 |
| H4b | 0.283 | 0.067 | 0.969 |
| H5a | −0.133 | 0.163 | 0.919 |
| H5b | −0.281 | −0.044 | 0.860 |

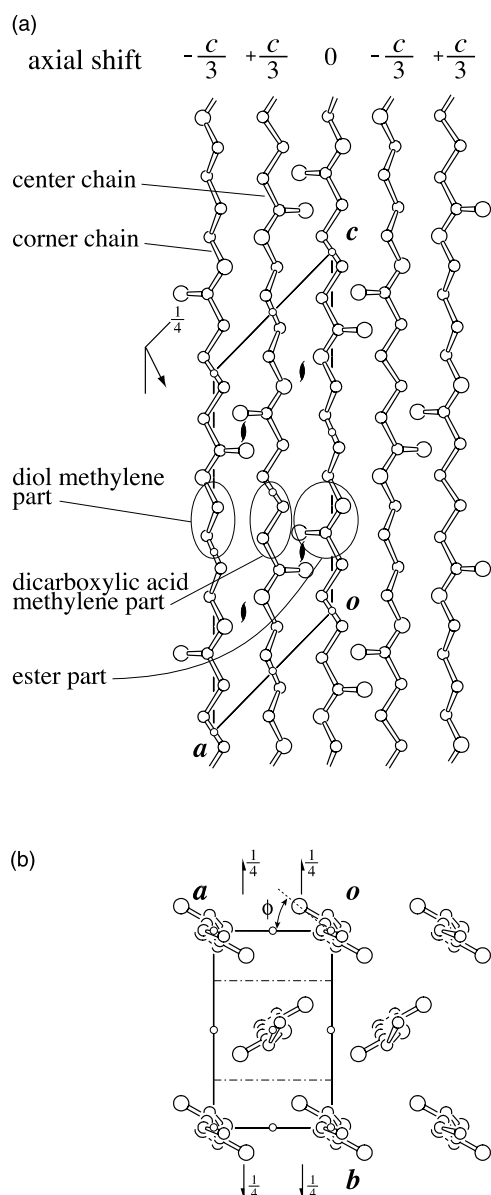


Fig. 3. Crystal structure of PTMA projected along the b -axis (a) and c -axis (b), together with graphical symbols of symmetry elements for the space group $P2_1/n$. All hydrogen atoms are omitted for simplicity. The setting angle of the polymer chain (ϕ) is defined as the angle between the a' -axis and the c -projected direction to the carbonyl oxygen from its molecular axis.

4. Results and discussion

4.1. Molecular structure

A conformation slightly distorted from the fully extended structure was obtained by the LALS refinement (Table 1). Only the torsional angle about the C2–O1 bond is significantly deviated from a trans value ($\theta_3 = 155^\circ$). Thus, the methylene segments in both the diol and dicarboxylic acid parts have almost planar structures and the molecular structure is twisted at the C2–O1 bond. This conformation is quite similar to that observed in the β form of PTMS [11]. On the other hand, a more distorted chain conformation of the α form of PTMA was reported by Pouget et al. [19]. In their model, the rotation about

the C2–O1 bond is also most deviated from trans and the conformation at this position is almost skew (122°). In addition, similar skew conformations were found at the corresponding position of poly(ethylene adipate) [31], poly(ethylene sebacate) [32,33] and poly(hexamethylene sebacate) [34]. The author thus tested a more deformed conformation than that above by restraining the angle θ_3 to a skew value during the refinement. After several refinement cycles, the model with the angle θ_3 of 123° showed $\Omega = 2.35 \times 10^4$, $R_w = 0.202$ and the shortest non-bonded interatomic distance of 0.214 nm (between H1a and H4a). This result indicates that the molecular model containing the skew conformation can roughly explain the observed intensity distribution of the fiber pattern. However, as mentioned above, our final structure is more reasonable in terms of both the X-ray fiber diffraction data and the intermolecular contacts. The different molecular conformation found in the present study may be due to not only the slightly longer observed fiber period of 1.442 nm than that of previous studies [13,14,19,20], but also the procedures of the structure determination. Pouget et al. [19] used both the X-ray fiber diffraction patterns of uniaxially oriented samples and the equatorial electron diffraction patterns obtained from solution-grown single crystals for their analysis on the α form of PTMA. The former were qualitatively compared with the simulated diffraction pattern to discard more divergent models. The latter were used to quantitatively evaluate the models by calculating R -factors during the refinement of the structure model. Since, the c -projected structure of our final model was similar to that containing the skew conformation, it seemed to be difficult to examine the difference in molecular structure using only the equatorial reflections. Indeed, the R -factors calculated using the equatorial reflections were 0.093 and 0.097 for the final and skew models, respectively. Therefore, in the present study, the relatively small discrepancy in the chain conformation could be identified based on all the reflection data from the equator to the 12th layer line.

4.2. Crystal structure

As mentioned in the structure analysis section, it was found that the space group $P2_1/n$ was most appropriate for crystals of the α form of PTMA, being consistent with that reported by Pouget et al. [19]. Moreover, the same space group was proposed for crystal structures of several poly(alkylene dicarboxylate)s, such as PTMS (α and β forms) [11], poly(hexamethylene sebacate) [35], poly(decamethylene sebacate) [36] and poly(ethylene adipate) (β -structure) [31]. Fig. 3 shows the projections of the crystal structure of the α form of PTMA viewed along the b - and c -axes. The neighboring chains along the a -axis direction are shifted approximately $-c/3$ ($=a \cos \beta = -0.484$ nm) along the c -axis according to the monoclinic cell dimensions. On the other hand, a shift of $+c/3$ along the c -axis occurs for neighboring chains along the [110] direction owing to the translation arising from the diagonal glide symmetry $[(a+c)/2]$. Because of such axial shifts between the adjacent chains, the methylene unit in diol and dicarboxylic acid segments, and ester segments are in turn

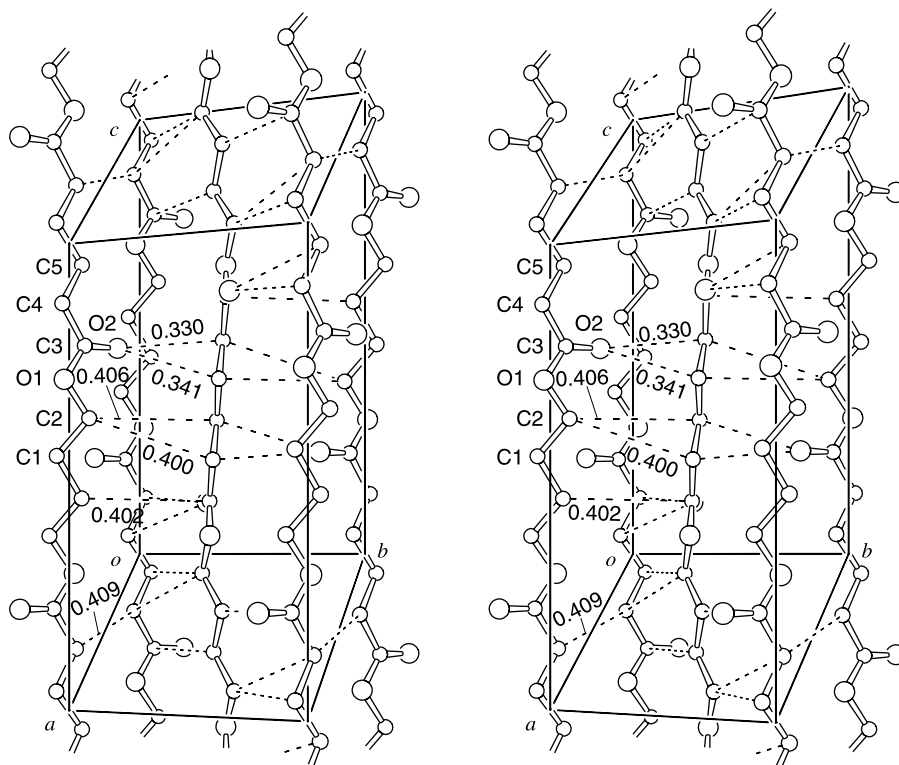


Fig. 4. Stereodrawing of the molecular packing of the α form of PTMA (drawn with ORTEP-III [41]). Broken lines indicate intermolecular distances less than 0.36 nm and 0.41 nm for C \cdots O and C \cdots C, respectively. All hydrogen atoms are omitted for simplicity.

arranged along the direction perpendicular to the bc -plane (Fig. 3(a)).

Some intermolecular distances less than 0.36 nm for C \cdots O and 0.41 nm for C \cdots C are shown in Fig. 4. Since, most of the intermolecular contacts in Fig. 4 were observed between corner and center chains in a unit cell, polyester chains are more closely packed along the [110] direction than the [100] direction. In addition, it was also found that carbonyl oxygen atoms of the corner chains are directed to the methylene segment in the center chain (Fig. 4). If the polyester chains had the fully extended conformation, the intermolecular distance between O2 and C4 atoms would have been 0.309 nm. While on the resultant structure, the O2 \cdots C4 distance is 0.330 nm owing to the molecular twist around the C2–O1 bond.

In a unit cell of the α form of PTMA, the position of the C=O group of the corner chain along the c -axis was close to that of the center chain (Fig. 3(a)). These C=O groups were related by the crystallographic 2 $_1$ -axes along the b -axis at $z=1/4$ and $z=3/4$. The total dipole moment arising from C=O groups is oriented in one direction at $z=1/4$, and in the opposite direction at $z=3/4$. Such a dipole arrangement seems to stabilize the crystal lattice of the α form of PTMA.

The α form of PTMA has the c -projected unit cell parameters of a' ($=a \sin \beta$) = 0.474 nm and b' ($=b$) = 0.790 nm. These projected cell dimensions are different from those of poly(alkylene dicarboxylate)s with comparatively long methylene segments, such as poly(hexamethylene

sebacate) [35], poly(decamethylene sebacate) [36], poly(tetramethylene dodecanoate) [37] and poly(hexamethylene dodecanoate) [34] ($a' \approx 0.50$ nm and $b' \approx 0.74$ nm), and the orthorhombic form of polyethylene ($a' = 0.4939$ nm and $b' = 0.7417$ nm) [38]. In addition, the setting angle (ϕ) of a polymer chain in the α form of PTMA (37°), which is defined as the angle between the a' -axis and the c -projected direction to the carbonyl oxygen from its molecular axis, is also slightly different from those of the poly(alkylene dicarboxylate)s (43 – 47°) [34–37] and polyethylene (45°) [38]. In the case of polyethylene, the ϕ is defined as the angle between the zigzag plane of the polymer chain and the a' -axis. It is interesting to note that the c -projected cell dimensions and the setting angle of the α form of PTMA are quite similar to those of 1:1 ethylene/carbon monoxide copolymer (1:1 E/CO copolymer) ($a' = 0.476$ nm, $b' = 0.797$ nm and $\phi = 39^\circ$) [39]. The crystal structure of 1:1 E/CO copolymer is isomorphous to that of the orthorhombic form of polyethylene and the C=O groups of two chains in the unit cell locate at the same height along the fiber axis. Since, the unit cell parameters and setting angles of E/CO copolymer become similar to those observed in polyethylene with an increasing ethylene/carbon monoxide ratio, the concentration of methylene segments and the relative location of the C=O groups of adjacent chains along its molecular axis seem to affect the lateral packing of polymer chains [40]. Therefore, the a' and b' cell dimensions and the angle ϕ found in the α form of PTMA would reflect the close arrangement of C=O groups between neighboring chains.

Recently, Pouget et al. [19] and Iwata et al. [20] independently analyzed the *c*-projected chain packing of the β form of PTMA based on the electron diffraction data obtained from solution-grown single crystals. They proposed essentially the same crystal structure model with unit cell dimensions of $a=0.503$ and $b=0.732$ nm, in which there were two chains having a planar zigzag conformation and the setting angle was 46° . These results suggest that the relative position between adjacent polymer chains along the fiber axis in the β form of PTMA is somewhat different from that in the α form. We would thus expect such a difference in the lateral packing to be closely related to the stability of both the crystal forms.

5. Conclusion

The crystal structure of the α form of PTMA was analyzed based on X-ray fiber diffraction data. A total of 103 independent diffraction spots up to a resolution of 0.11 nm were observed using the synchrotron radiation source (SPring-8, BL40B2). All the observed reflections could be indexed in terms of a monoclinic cell with the parameters of $a=0.6776(6)$, $b=0.7904(6)$, c (fiber axis)= $1.442(1)$ nm and $\beta=135.6(1)^\circ$. Crystals of the α form belong to the monoclinic system of space group $P2_1/n$ and the final *R*-factor in the present analysis was 0.130. The molecular structure of the α form was slightly deformed from the fully extended conformation. Only the torsional angle C1–C2–O1–C3 was significantly deviated from a trans value (155°). Thus, the methylene segments in both the diol and dicarboxylic acid parts had almost planar structures and the molecular structure was twisted in the ester part. The molecular conformation was distorted so as to avoid too short intermolecular contact between the corner and center chains in a unit cell. The C=O groups of the corner and center chains were closely located along the *c*-axis and were related by the crystallographic 2_1 -axes along the *b*-axis at $z=1/4$ and $z=3/4$. The total dipole moment arising from the C=O groups was oriented in one direction at $z=1/4$, and in the opposite direction at $z=3/4$. Such a dipole arrangement seemed to stabilize the crystal lattice of the α form of PTMA. In addition, the relative distance between C=O groups of neighboring chains along the fiber axis would affect the *c*-projected unit cell dimensions (a' and b') and the setting angle (ϕ) of the polymer chain. Since, the values of a' , b' and ϕ of the β form of PTMA were different from those of the α form, the arrangement of C=O groups along the fiber axis in the β form was somewhat different from that in the α form. Such a difference in lateral packing would be closely related to the stability of both the crystal forms.

Acknowledgements

The synchrotron radiation experiments were performed at BL40B2 in SPring-8 with the approval of the Japan Synchrotron Radiation Research Institute (JASRI) (Proposal No. 2001A0236-NDL-np). This research was partially supported by a Grant-in-aid for Scientific Research (09750984)

from the Ministry of Education, Science, Sports, Science and Technology of Japan.

Supplementary data

Supplementary data associated with this article can be found, in the online version, at doi:10.1016/j.polymer.2005.09.010

References

- [1] Mochizuki M, Mukai K, Yamada K, Ichise N, Murase S, Iwaya Y. *Macromolecules* 1997;30(24):7403–7.
- [2] Nishida H, Tokiwa Y. *J Environ Polym Degrad* 1993;1(3):227–33.
- [3] Nishida H, Tokiwa Y. *Chem Lett* 1994;(7):1293–6.
- [4] Pranamuda H, Tokiwa Y, Tanaka H. *Appl Environ Microbiol* 1995;61(5):1828–32.
- [5] Tokiwa Y, Suzuki T, Takeda K. *Agric Biol Chem* 1986;50(5):1323–5.
- [6] Takiyama E, Fujimaki T. 'BIONOLE' biodegradable plastic through chemical synthesis. In: Doi Y, Fukuda K, editors. *Biodegradable plastics and polymers*, vol. 12. Amsterdam: Elsevier; 1994. p. 150–74. Part 3.
- [7] Nishioka M, Tuzuki T, Wanajyo Y, Oonami H, Horiuchi T. Biodegradation of 'BIONOLE'. In: Doi Y, Fukuda K, editors. *Biodegradable plastics and polymers*, vol. 12. Amsterdam: Elsevier; 1994. p. 584–90. Part 3.
- [8] Ichikawa Y, Suzuki J, Washiyama J, Moteki Y, Noguchi K, Okuyama K. *Polymer* 1994;35(15):3338–9.
- [9] Ichikawa Y, Washiyama J, Moteki Y, Noguchi K, Okuyama K. *Polym J* 1995;27(12):1230–8.
- [10] Ichikawa Y, Washiyama J, Moteki Y, Noguchi K, Okuyama K. *Polym J* 1995;27(12):1264–6.
- [11] Ichikawa Y, Kondo H, Igarashi Y, Noguchi K, Okuyama K, Washiyama J. *Polymer* 2000;41(12):4719–27.
- [12] Ichikawa Y, Noguchi K, Okuyama K, Washiyama J. *Polymer* 2001;42(8):3703–8.
- [13] Minke R, Blackwell J. *J Macromol Sci, Phys* 1979;B16(3):407–17.
- [14] Minke R, Blackwell J. *J Macromol Sci, Phys* 1980;B18(2):233–55.
- [15] Gan Z, Abe H, Doi Y. *Macromol Chem Phys* 2002;203(16):2369–74.
- [16] Gan Z, Kuwabara K, Abe H, Iwata T, Doi Y. *Biomacromolecules* 2004;5(2):371–8.
- [17] Gan Z, Kuwabara K, Abe H, Iwata T, Doi Y. *Polym Degrad Stab* 2005;87(1):191–9.
- [18] Kuwabara K, Gan Z, Nakamura T, Abe H, Doi Y. *Polym Degrad Stab* 2004;84(1):105–14.
- [19] Pouget E, Almontassir A, Casas MT, Puiggali J. *Macromolecules* 2003;36(3):698–705.
- [20] Iwata T, Kobayashi S, Tabata K, Yonezawa N, Doi Y. *Macromol Biosci* 2004;4(3):296–307.
- [21] Kondo H, Ichikawa Y, Noguchi K, Okuyama K. *Polym Preprint Jpn Eng Ed* 1997;46(1):E212.
- [22] Okuyama K, Noguchi K, Miyazawa T, Yui T, Ogawa K. *Macromolecules* 1997;30(19):5849–55.
- [23] Okuyama K, Obata Y. *Polym Preprint Am Chem Soc* 1992;(33):280.
- [24] Obata Y, Okuyama K. *Kobunshi Ronbunshu* 1994;51:371–8.
- [25] Kahn R, Fourme R, Gadet A, Janin J, Dumas C, André D. *J Appl Cryst* 1982;15(3):330–7.
- [26] Smith PJC, Arnott S. *Acta Crystallogr* 1972;A34(1):3–11.
- [27] Cromer DT, Waber JT, editors. *International tables for crystallography*. Birmingham: Kynoch Press; 1974. p. 71–4.
- [28] Okada K, Noguchi K, Okuyama K, Arnott S. *Comput Biol Chem* 2003;27(3):265–85.
- [29] Allen FH. *Acta Crystallogr* 2002;B58(3):380–8.

- [30] Hahn T, editor. International tables for crystallography, a, space-groups symmetry. Dordrecht: D. Reidel Publishing Company; 1983. p. 81–90.
- [31] Turner-Jones A, Bunn CW. *Acta Crystallogr* 1962;15(2):105–13.
- [32] Kanamoto T, Tanaka K, Nagai H. *J Polym Sci A-2* 1971;9(11):2043–60.
- [33] Hobbs SY, Billmeyer Jr FW. *J Polym Sci A-2* 1969;7(6):1119–21.
- [34] Gestí S, Almontassir A, Casas MT, Puiggali J. *Polymer* 2004;45(26):8845–61.
- [35] Armelin E, Casas MT, Puiggali J. *Polymer* 2001;42(13):5695–9.
- [36] Armelin E, Almontassir A, Franco L, Puiggali J. *Macromolecules* 2002;35(9):3630–5.
- [37] Almontassir A, Gestí S, Franco L, Puiggali J. *Macromolecules* 2004;37(14):5300–9.
- [38] Takahashi Y. *Macromolecules* 1998;31(12):3868–71.
- [39] Chatani Y, Takizawa T. *J Polym Sci* 1961;55:811–9.
- [40] Chatani Y, Takizawa T, Murahashi S. *J Polym Sci* 1962;62:S27–S30.
- [41] Burnett MN, Johnson CK. ORTEP-III, report ORNL-6895. Oak Ridge, TN: Oak Ridge National Laboratory; 1996.